Supplementary information for

Sensitivity of PM2.5 mass to ammonia and nitrate availability in Hong Kong

Zijing ZHANG[1] and Jian Zhen YU[1,2*]

1 Division of Environment and Sustainability, Hong Kong University of Science and Technology, Clearwater Bay, Kowloon, Hong Kong

2 Department of Chemistry, Hong Kong University of Science and Technology, Clearwater Bay, Kowloon, Hong Kong

**Corresponding author: jian.yu@ust.hk*

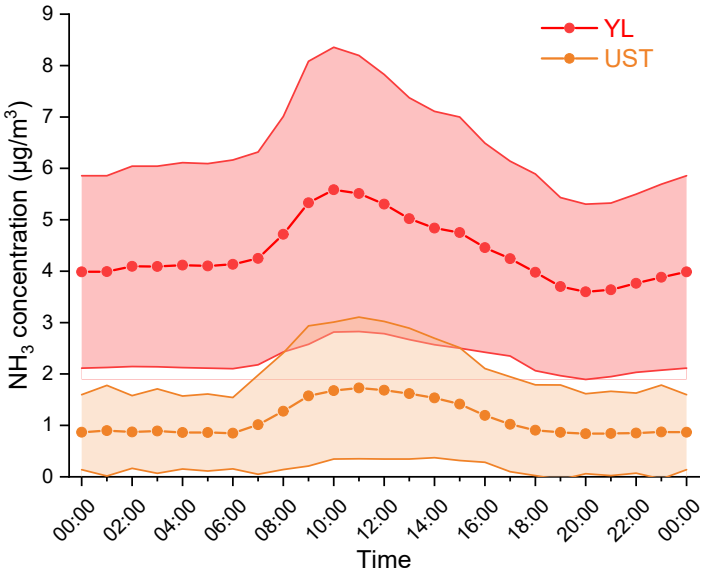

Fig. S1 Diurnal trend of gaseous NH_3 concentration in YL site and UST site (mean value ± 1σ)

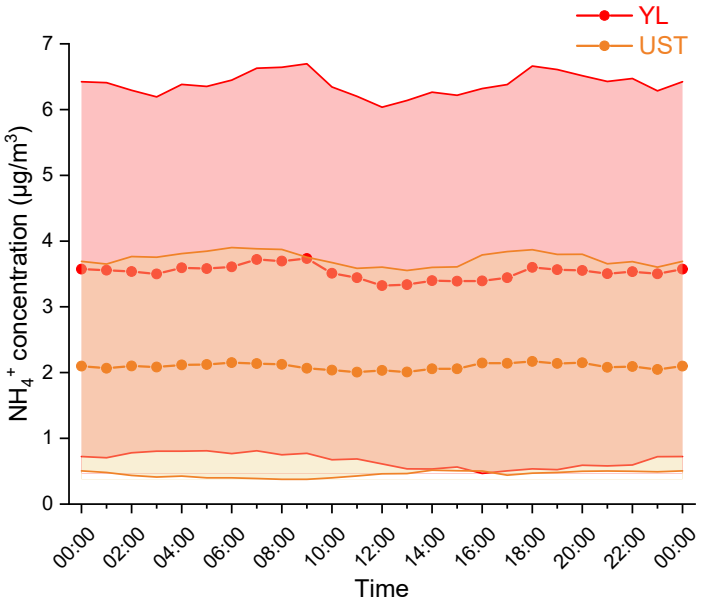

Fig. S2 Diurnal trend of particulate NH_4^+ concentration in YL site and UST site (mean value ± 1σ)

Section S1. MARGA data validation

To ensure the accuracy of measurement, MARGA was calibrated with standard cation and anion solutions every two to three months. Moreover, filter sampling was conducted at the same site from January to December in 2016 to serve as a reference for MARGA data. Results showed a good correlation between filter and MARGA measurements of sulfate and ammonium (Fig. S3 a, b). However, the correlation of nitrate was not so good as sulfate and ammonium due to sampling artifacts of filter measurement like volatility-induced loss, especially when the nitrate concentration was low (Fig. S3 c). Overall, the results of filter measurements during the whole year of 2016 provide evidence for the reliability of MARGA data.

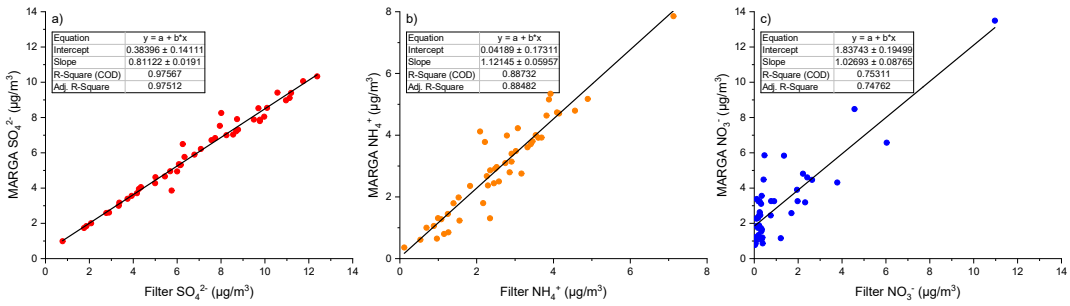

Fig.S3 Comparison between measurements by filters and MARGA during Jan. to Dec.2016 of a)

SO_4^{2-}, b) NH_4^+ and c) NO_3^-

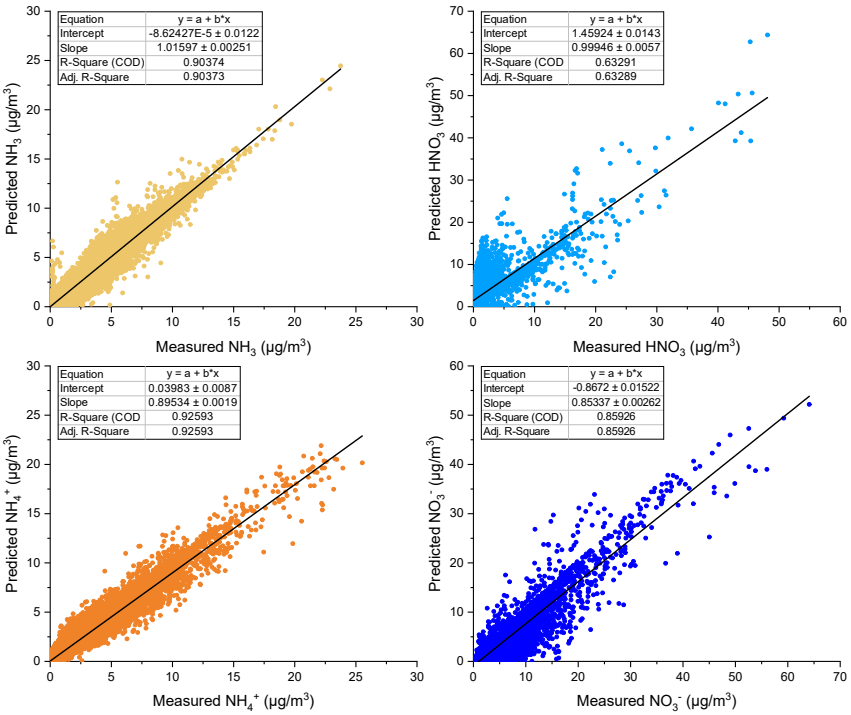

Fig.S4 Comparison between measured and predicted NH_3, NH_4^+, HNO_3, NO_3^-.

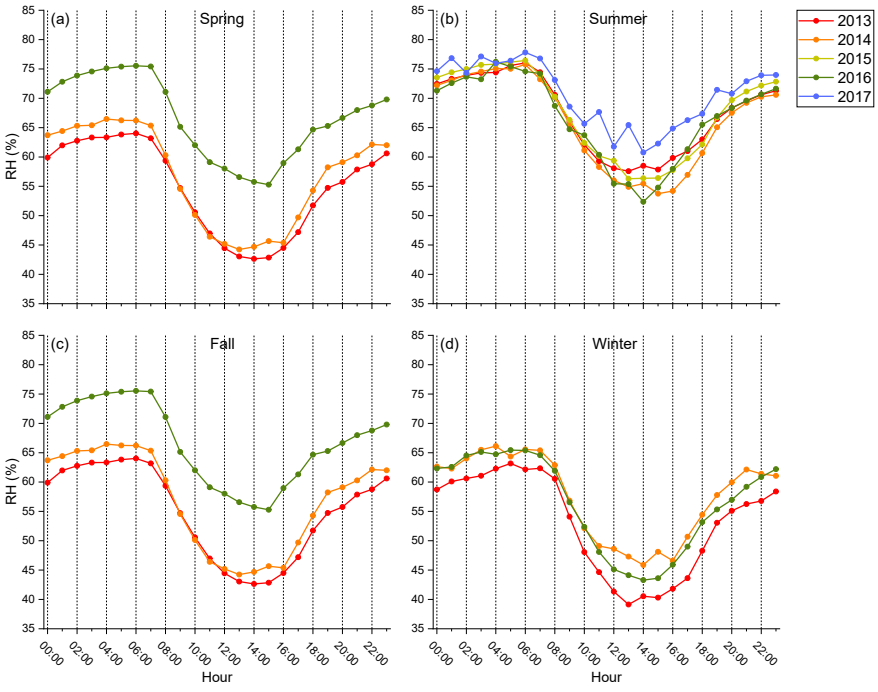

Fig. S5 Diurnal trend of relative humidity during (a) Spring, (b) Summer, (c) Fall, (d) Winter from

2013 to 2017

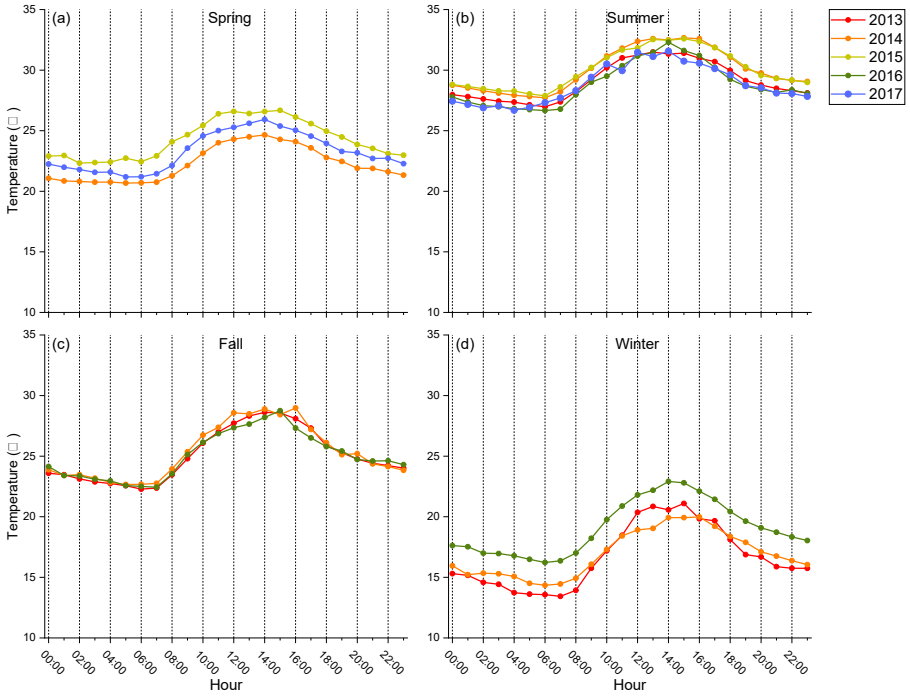

Fig. S6 Diurnal trend of temperature during (a) Spring, (b) Summer, (c) Fall, (d) Winter from 2013 to 2017

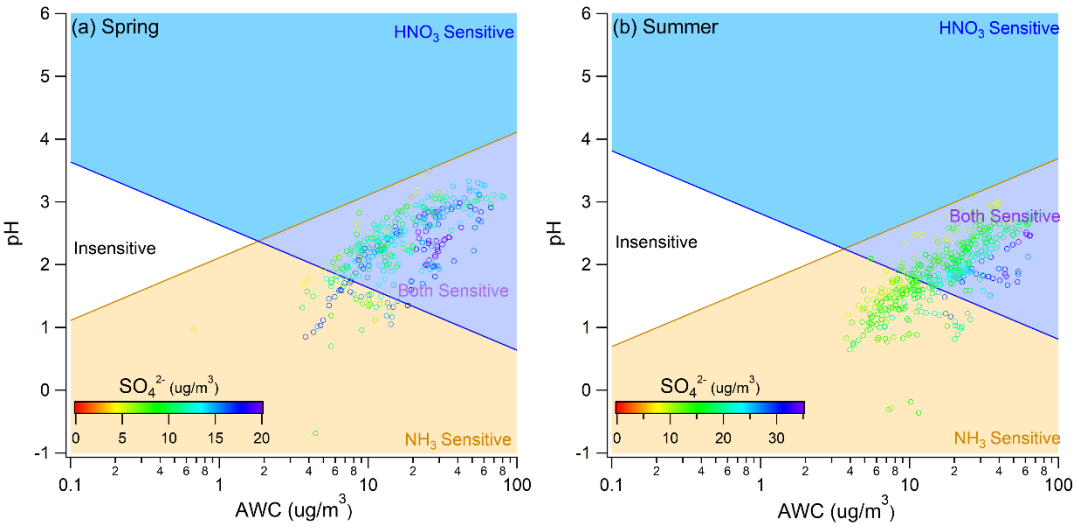

Fig. S7 The sensitivity regime plot of data points colored by sulfate concentration under polluted conditions in (a) spring and (b) summer.

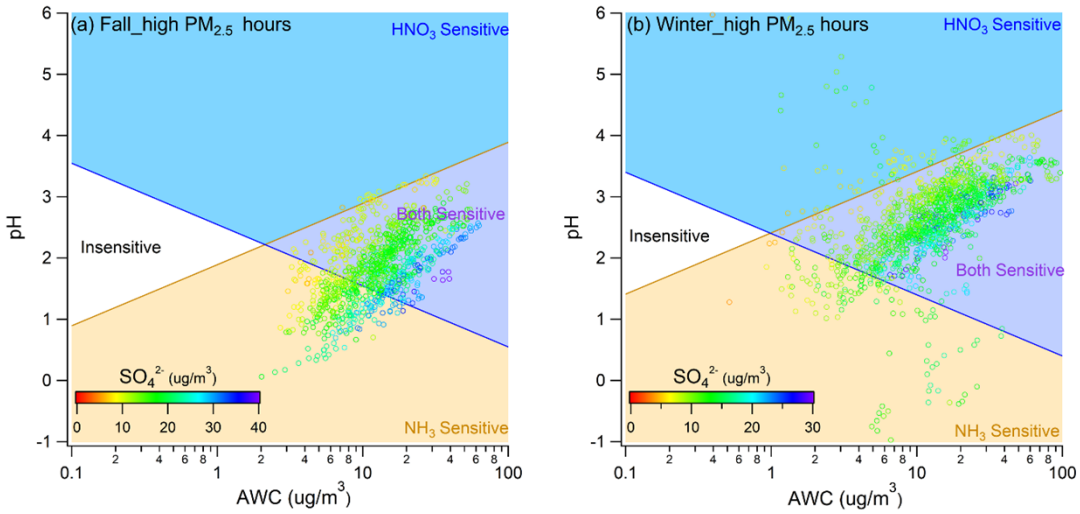

Fig. S8 The sensitivity regime plot of data points colored by sulfate concentration under polluted conditions in (a) fall and (b)winter.

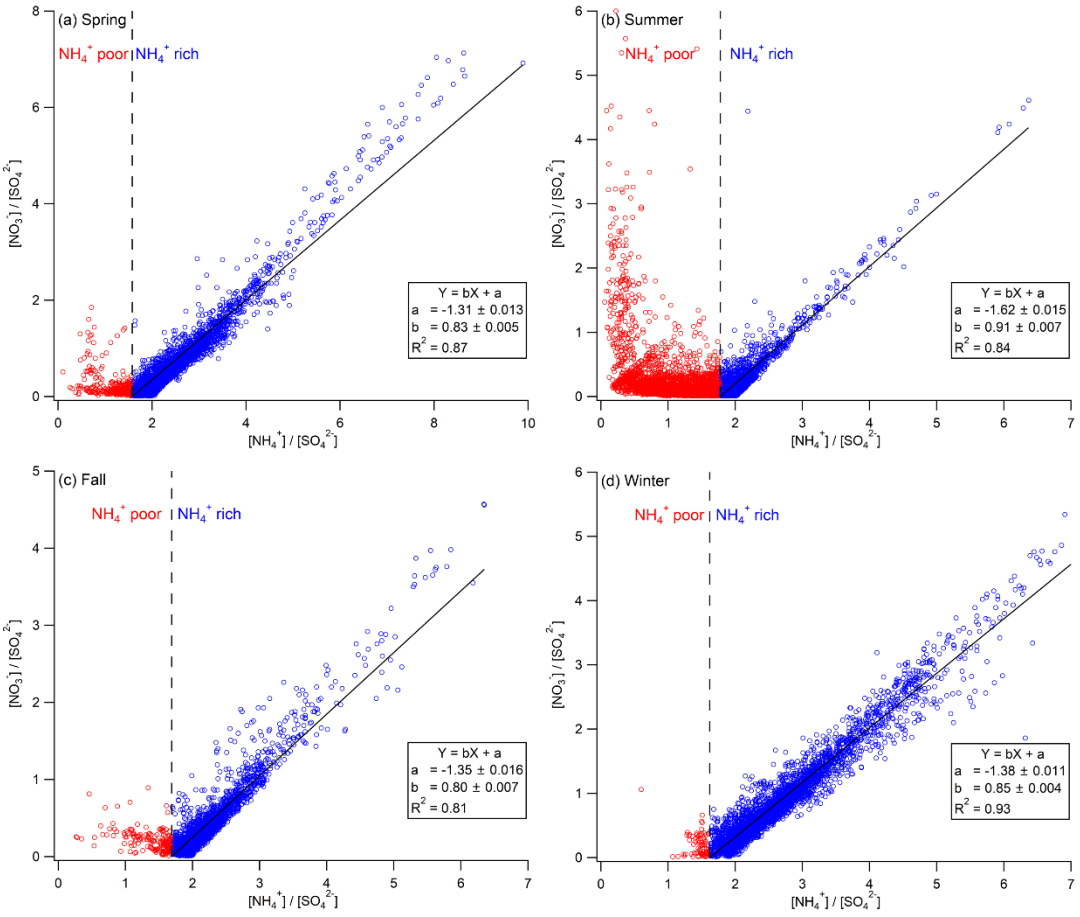

Fig. S9 Correlation plot between molar ratio of $[NO_3^-]/[SO_4^{2-}]$ and $[NH_4^+]/[SO_4^{2-}]$ in (a) spring, (b) summer, (c) fall, (d) winter.

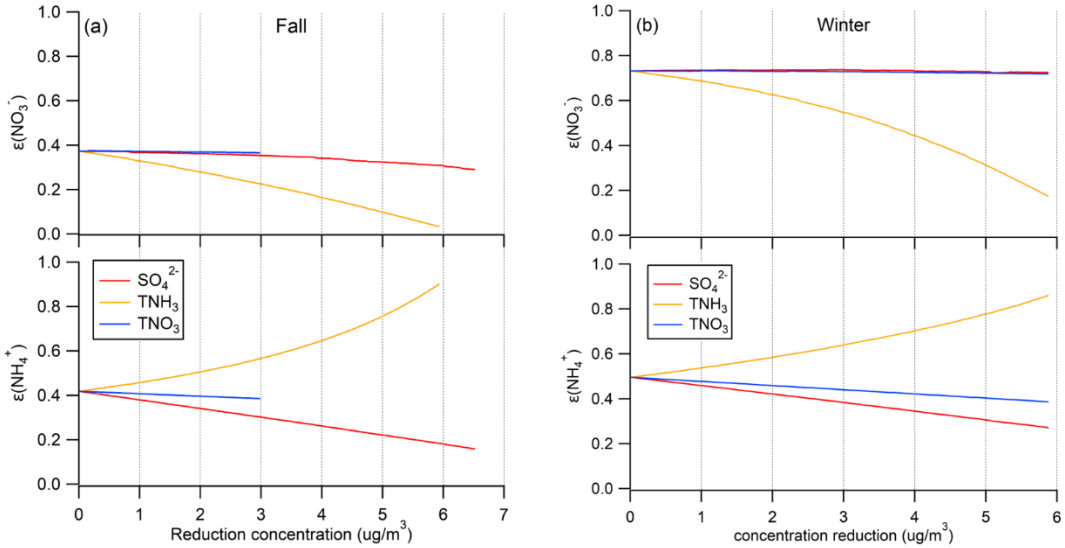

Fig. S10 Variation of $\varepsilon(NO_3^-)$ and $\varepsilon(NH_4^+)$ with the reduction of sulfate, TNH_3 and TNO_3.

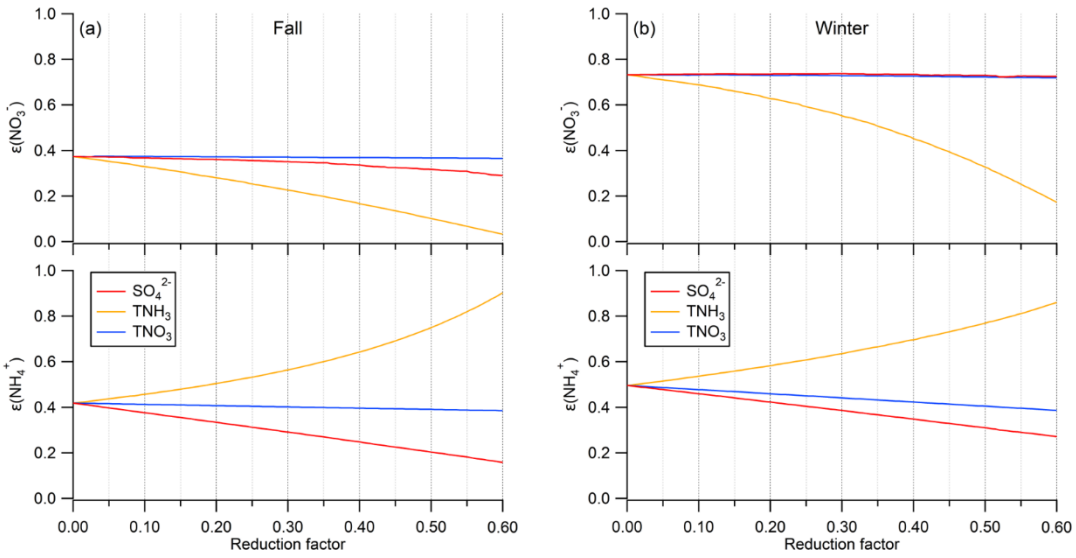

Fig. S11 Variation of $\varepsilon(NO_3^-)$ and $\varepsilon(NH_4^+)$ with the reduction percentage of sulfate, TNH_3 and TNO_3.

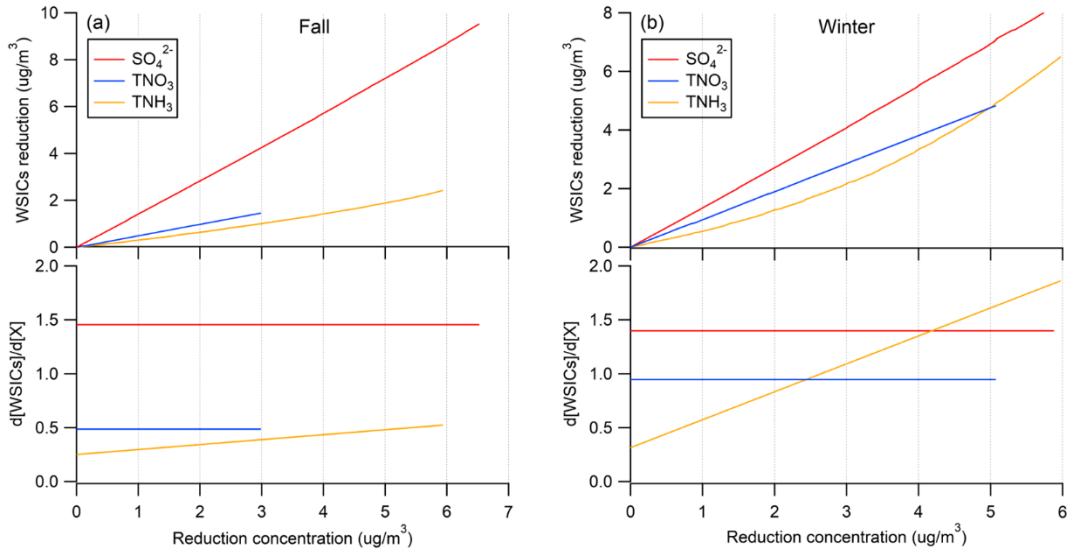

Fig. S12 The efficiency of controlling sulfate, TNO_3, TNH_3 in reducing total WSICs concentration during a) fall and b) winter. Top: the reduction of WSICs concentration vs. the reduction concentration of TNH_3, TNO_3 or sulfate. Bottom: The derivative of the lines in the top plot.